The stretch to stray on time: Resonant length of random walks in a transient

Martin Falcke[1,2,a)] and Victor Nicolai Friedhoff[1,2,b)]

[1]*Max Delbrück Center for Molecular Medicine, Robert Rössle Str. 10, 13125 Berlin, Germany*
[2]*Department of Physics, Humboldt University, Newtonstr. 15, 12489 Berlin, Germany*

First-passage times in random walks have a vast number of diverse applications in physics, chemistry, biology, and finance. In general, environmental conditions for a stochastic process are not constant on the time scale of the average first-passage time or control might be applied to reduce noise. We investigate moments of the first-passage time distribution under an exponential transient describing relaxation of environmental conditions. We solve the Laplace-transformed (generalized) master equation analytically using a novel method that is applicable to general state schemes. The first-passage time from one end to the other of a linear chain of states is our application for the solutions. The dependence of its average on the relaxation rate obeys a power law for slow transients. The exponent ν depends on the chain length N like $\nu = -N/(N+1)$ to leading order. Slow transients substantially reduce the noise of first-passage times expressed as the coefficient of variation (CV), even if the average first-passage time is much longer than the transient. The CV has a pronounced minimum for some lengths, which we call resonant lengths. These results also suggest a simple and efficient noise control strategy and are closely related to the timing of repetitive excitations, coherence resonance, and information transmission by noisy excitable systems. A resonant number of steps from the inhibited state to the excitation threshold and slow recovery from negative feedback provide optimal timing noise reduction and information transmission. © *2018 Author(s).*
All article content, except where otherwise noted, is licensed under a Creative Commons Attribution (CC BY) license (http://creativecommons.org/licenses/by/4.0/).
https://doi.org/10.1063/1.5023164

Given the randomness of a process, many applications ask for the time when a state is passed first. First-passage times of random walks comprising several steps exhibit typically a standard deviation larger than 80% of the average. Are there simple means to render these processes more precise? We show that these relative fluctuations can be reduced by one order of magnitude by applying a relaxational transient and are minimal at optimal lengths, which we call resonant lengths. This is simple and efficient noise control applicable to random walks in all disciplines. It works reliably for Markovian and non-Markovian systems. This new phenomenon of a robust resonance between a relaxation rate and a random walk length is closely related to coherence resonance in excitable systems.

I. INTRODUCTION

Continuous-time random walks are a unifying concept across physics,[1–14] chemistry,[15–17] biology,[18–21] and finance.[22,23] The drunkard's straying on his way home from the pub is the graphic example frequently used to illustrate the randomness of step timing and direction. In particular, the time of first passage of a specific state given the stochastic nature of the process is of interest in many applications. It describes the time the drunkard arrives home, the time

necessary for a chemical reaction or gene expression to reach a certain number of product molecules,[15,21] or a quantity in one of the many other applications.[2,3,12,17,24–37]

While noise happens on the small length scales and short time scales of a system, it may trigger events on a global scale. One of the most important functions of noise for macroscopic dynamics arises from its combination with thresholds.[38–40] These are defined by the observation that the dynamics of a system remains close to a stable state as long as it does not cross the threshold value, and an actively amplified deviation from this state happens when it is crossed. Noise drives the system across the threshold in a random manner. First passage is a natural concept to describe the timing of threshold crossings. Ignition processes are an illustrative example. Although a small random spark might not be capable of igniting an inflammable material, a few of them might cause an explosion or forest fire. If the system again attains its stable state upon recovery from a deviation, such behavior is called excitable and the large deviation is an excitation. The excitation is terminated by negative feedback. A forest is excitable, because it regrows after a fire. Consumption of inflammable trees acts as the negative feedback. Excitability describes not only forest fires but also the dynamics of heterogeneous catalysis,[41] the firing of neurons,[42] the properties of heart muscle tissue,[42] and many other systems in physics, chemistry, and biology.[43–47]

Random walks are frequently defined on a set of discrete states. The rates $f_{i,j}$ or waiting-time distributions $\Psi_{i,j}$ for transitions from state i to j set the state dwell times. The first-

a)Martin.Falcke@mdc-berlin.de
b)Nicolai.Friedhoff@mdc-berlin.de

passage time between two widely separated states is much longer than the individual dwell times, and the conditions setting the rates and parameters of the $\Psi_{i,j}$ are likely to change or external control acts on the system between start and first passage. The conditions for igniting a forest fire change with the seasons or because the forest recovers from a previous fire. The occurrence of subcritical sparks during recovery has essentially no effect on the process of regrowth. More generally, noise does not affect the recovery on large length and long time scales, and the random process experiences recovery as a slow deterministic change of environmental conditions. Since recovery is typically a slow relaxation process,[45–47] it dominates event timing. Hence, first passage in an exponential transient is a natural concept through which one can understand the timing of sequences of excitations. We will investigate it in this study.

We will take Markovian processes as one of the asymptotic cases of transient relaxation. Non-Markovian waiting-time distributions are also used in many applications. They arise naturally in diffusion and transport theory.[1,3,5–8,30,48–51] Frequently, in biological applications, we face lumped states consisting of many "microscopic" states.[52–54] Transitions between lumped states are non-Markovian owing to the internal dynamics. We may also use waiting-time distributions if we lack information on all the individual steps of a process, but we do know the inter-event interval distributions. This is usually the case with the stimulation of a cell and the appearance of a response,[55] or differentiation sequences of stem cells.[37] The state probabilities of non-Markovian processes obey generalized master equations, which we will use here.[10,16,56–59]

In Sec. II, we present a formulation of the general problem in terms of the normal and generalized master equations and give analytic solutions for both of these. These solutions apply to general state schemes. We continue with investigating first passage on linear chains of states in Sec. III. We present results on scaling of the average first-passage time with the relaxation rate of the transient γ and the chain length N in Sec. IV, and results on the phenomenon of resonant lengths in Sec. V.

II. BASIC EQUATIONS

A. The asymptotically Markovian master equation

In this section, we consider transition rates relaxing with rate γ to an asymptotic value $\lambda_{i,j}$ like

$$f_{i,j}(t) = \lambda_{i,j}\left(1 + B_{i,j}e^{-\gamma t}\right), \quad \lambda_{i,j} \geq 0, \, B_{i,j} \geq -1. \quad (1)$$

They reach a Markov process asymptotically. The dynamics of the probability $P_{i,j}(t)$ to be in state j for a process that started in i at $t = 0$ obey the master equation

$$\frac{dP_{i,j}}{dt} = \sum_{k=0}^{N} \lambda_{k,j}P_{i,k} - \lambda_{j,k}P_{i,j} + e^{-\gamma t}\left(\lambda_{k,j}B_{k,j}P_{i,k} - \lambda_{j,k}B_{j,k}P_{i,j}\right). \quad (2)$$

In matrix notation with the vector of probabilities P_i, we have

$$\frac{dP_i}{dt} = EP_i + e^{-\gamma t}DP_i, \quad (3)$$

with the matrices E and D defined by Eq. (2). The initial condition defines the vector $r_i = \{\delta_{ij}\}, j = 0,\ldots,N$. The Laplace transform of the master equation allows for a comfortable calculation of moments of the first-passage times, which we will carry out in Sec. III. The Laplace transform of Eq. (3) is the system of linear difference equations

$$s\tilde{P}_i(s) - r_i = E\tilde{P}_i(s) + D\tilde{P}_i(s + \gamma). \quad (4)$$

B. The generalized master equation

1. The waiting-time distributions

Waiting-time distributions $\Psi_{j,k}$ in a constant environment depend on the time $t - t'$ elapsed since the process entered state j at time t'. The change in conditions causes an additional dependence on t: $\Psi_{j,k}(t, t - t')$. The lumping of states, which we introduced as a major cause of dwell-time-dependent transition probabilities, often entails $\Psi_{j,k}(t, 0) = \Psi_{j,k}(t, \infty) = 0$, with a maximum of $\Psi_{j,k}(t, t - t')$ at intermediate values of $t - t'$.[60] Waiting-time distributions used in transport theory exhibit similar properties.[30,49,50,61] We use a simple realization of this type of distributions by a biexponential function in $t - t'$

$$\Psi_{j,k}(t, t - t') = A_{j,k}\left(e^{-\alpha_{j,k}(t-t')} - e^{-\beta_{j,k}(t-t')}\right)$$
$$\times \left(1 + M_{j,k}e^{-\gamma t}\right) \quad (5)$$
$$= g_{j,k}(t - t') + h_{j,k}(t - t')e^{-\gamma t}. \quad (6)$$

The transient parts $h_{j,k}(t - t')e^{-\gamma t}$ of $\Psi_{j,k}(t, t - t')$ collect all factors of $e^{-\gamma t}$ in Eq. (5). The functions $g_{j,k}(t - t')$ describe the asymptotic part of the waiting-time distributions remaining after the transient. The $\Psi_{j,k}(t, t - t')$ are normalized to the splitting probabilities $C_{j,k} = \int_{t'}^{\infty} dt\, \Psi_{j,k}(t, t - t')$ (the total probability for a transition from j to k given the system entered j at t'). They satisfy

$$\sum_{k=0}^{N} C_{j,k}(t') = 1. \quad (7)$$

2. The generalized master equation and its Laplace transform

In the non-Markovian case, the dynamics of the probabilities $P_{i,j}(t)$ obey a generalized master equation[62–66]

$$\frac{dP_{i,j}(t)}{dt} = \sum_{l=0}^{N} I_{l,j}(t) - \sum_{l=0}^{N} I_{j,l}(t), \quad (8)$$

where $I_{l,j}(t)$ is the probability flux due to transitions from state l to j given that the process started at state i at $t = 0$. The fluxes are the solutions of the integral equation

$$I_{l,j}(t) = \int_0^t dt'\, \Psi_{l,j}(t, t - t') \sum_{k=0}^{N} I_{k,l}(t') + q_{l,j}(t). \quad (9)$$

The second factor in the convolution is the probability of arriving in state l at time t', and the first factor is the

probability of leaving toward j at time t given arrival at t'. The $q_{l,j}$ are the initial fluxes, with $q_{l,j}(t) \equiv 0$ for $i \neq l$.

The Laplace transform of the probability dynamics equation (8) is

$$s\tilde{P}_{i,j}(s) - \delta_{ij} = \sum_{l=0}^{N} \tilde{I}_{l,j}(s) - \sum_{l=0}^{N} \tilde{I}_{j,l}(s), \qquad (10)$$

which contains the Laplace-transformed probability fluxes $\tilde{I}_{l,j}$. The Kronecker delta δ_{ij} captures the initial condition.

Laplace-transforming Eq. (9) is straightforward for terms containing the asymptotic part $g_{l,j}(t - t')$ of the $\Psi_{l,j}(t, t - t')$ [see Eq. (6)], since they depend on $t - t'$ only and the convolution theorem applies directly. The terms containing the transient part $h_{l,j}(t - t')e^{-\gamma t}$ depend on both $t - t'$ and t and require a little more attention

$$\int_0^\infty dt\, e^{-st} \int_0^t dt'\, h_{l,j}(t - t')e^{-\gamma t} \sum_{k=0}^{N} I_{k,l}(t')$$

$$= \int_0^\infty dt\, e^{-(s+\gamma)t} \int_0^t dt'\, h_{l,j}(t - t') \sum_{k=0}^{N} I_{k,l}(t')$$

$$= \tilde{h}_{l,j}(s + \gamma) \sum_{k=1}^{N} \tilde{I}_{k,l}(s + \gamma). \qquad (11)$$

This leads to the Laplace transform of Eq. (9)

$$\tilde{I}_{l,j}(s) = \tilde{q}_{l,j}(s) + \tilde{g}_{l,j}(s) \sum_{k=0}^{N} \tilde{I}_{k,l}(s)$$

$$+ \tilde{h}_{l,j}(s + \gamma) \sum_{k=0}^{N} \tilde{I}_{k,l}(s + \gamma). \qquad (12)$$

We write the $\tilde{I}_{l,j}(s)$ and $\tilde{q}_{l,j}(s)$ as vectors. In the most general case allowing transitions between all states, the vector $\tilde{I}(s)$ is

$$\tilde{I}(s) = \{\tilde{I}_{0,1}, \ldots, \tilde{I}_{0,N}, \tilde{I}_{1,0}, \ldots, \tilde{I}_{1,N}, \ldots, \tilde{I}_{N,0}, \ldots, \tilde{I}_{N,N-1}\} \quad (13)$$

and $\tilde{q}(s)$ accordingly. We obtain

$$\tilde{I}(s) = \tilde{G}(s)\tilde{I}(s) + \tilde{H}(s + \gamma)\tilde{I}(s + \gamma) + \tilde{q}(s). \qquad (14)$$

Solving for $\tilde{I}(s)$ results in

$$\tilde{I}(s) = \left[\mathbb{1} - \tilde{G}(s)\right]^{-1} \left[\tilde{H}(s + \gamma)\tilde{I}(s + \gamma) + \tilde{q}(s)\right]. \qquad (15)$$

This is again a system of linear difference equations. The entries in the matrices $\tilde{G}(s)$ and $\tilde{H}(s)$ are the functions $\tilde{g}_{l,j}(s)$ and $\tilde{h}_{l,j}(s)$, which are the Laplace transforms of $g_{l,j}(t - t')$ and $h_{l,j}(t - t')$ [Eq. (6)].

3. Solving the Laplace-transformed generalized and asymptotically Markovian master equations

All elements of $\tilde{H}(s)$ [Eq. (15)] vanish for $s \to \infty$. We also expect $\tilde{I}(s)$ to be bounded for $s \to \infty$. Hence, the solution for $\gamma = \infty$ is

$$\tilde{I}_\infty(s) = \left[\mathbb{1} - \tilde{G}(s)\right]^{-1} \tilde{q}(s). \qquad (16)$$

Consequently, if we obtain large Laplace arguments because of $k\gamma \gg 1$ instead of $\gamma = \infty$,

$$\tilde{I}(s + k\gamma) \approx \left[\mathbb{1} - \tilde{G}(s + k\gamma)\right]^{-1} \tilde{q}(s + k\gamma)$$

holds for the solution $\tilde{I}(s)$ for all values of $\gamma > 0$ and for k a natural number. Once we know $\tilde{I}(s + k\gamma)$, we can use Eq. (15) to find $\tilde{I}(s + (k - 1)\gamma)$

$$\tilde{I}(s + (k - 1)\gamma) \approx \left[\mathbb{1} - \tilde{G}(s + (k - 1)\gamma)\right]^{-1}$$
$$\times \{\tilde{H}(s + k\gamma)\left[\mathbb{1} - \tilde{G}(s + k\gamma)\right]^{-1} \tilde{q}(s + k\gamma)$$
$$+ \tilde{q}(s + (k - 1)\gamma)\}, \quad k \gg \gamma^{-1}. \qquad (17)$$

In this way, we can consecutively use Eqs. (15) and (17) to express $\tilde{I}(s + (k - j)\gamma)$, $j = 0, \ldots, k$, by known functions. The solution becomes exact with $k \to \infty$. With the definition $\tilde{A}(s) = \left[\mathbb{1} - \tilde{G}(s)\right]^{-1}\tilde{H}(s + \gamma)$, we obtain

$$\tilde{I}(s) = \left[\mathbb{1} - \tilde{G}(s)\right]^{-1}\tilde{q}(s)$$
$$+ \sum_{k=1}^{\infty} \prod_{j=0}^{k-1} \tilde{A}(s + j\gamma)\left[\mathbb{1} - \tilde{G}(s + k\gamma)\right]^{-1}\tilde{q}(s + k\gamma) \quad (18)$$

as the solution of Eq. (15). Equation (18) is confirmed by verifying that it provides the correct solution in the limiting cases $\gamma = 0$ and $\gamma = \infty$. In the latter, all entries of the matrix $\tilde{H}(s)$ vanish, and we obtain directly the result without transient, Eq. (16). For $\gamma = 0$, we notice that

$$\sum_{k=1}^{\infty} \prod_{j=0}^{k-1} \tilde{A}(s) = \{\mathbb{1} - \left[\mathbb{1} - \tilde{G}(s)\right]^{-1}\tilde{H}(s)\}^{-1} - \mathbb{1}$$

holds, which leads to the correct solution of Eq. (15)

$$\tilde{I}(s) = \left[\mathbb{1} - \tilde{G}(s) - \tilde{H}(s)\right]^{-1}\tilde{q}(s). \qquad (19)$$

Formally, Eq. (18) is a solution of Eq. (15) for general $\tilde{H}$. Requiring convergence of the solution entails conditions on the matrices. The sum in Eq. (18) converges if γ is larger than 0, and there is a value s_1, such that the modulus of all eigenvalues of $\tilde{A}(s)$ is smaller than 1 for $s > s_1$. This holds, since the entries of $\tilde{G}$ and $\tilde{H}$ are Laplace transforms (see also Appendix B).

We now turn to the asymptotically Markovian master equation (2) and write its Laplace transform (4) as

$$\tilde{P}_i(s) = (\mathbb{1}s - E)^{-1}\left[D\tilde{P}_i(s + \gamma) + r_i\right]. \qquad (20)$$

This equation has the same structure as Eq. (15), and since the matrix $(\mathbb{1}s - E)^{-1}$ also vanishes for $s \to \infty$, we can calculate the Laplace transform of the $P_{i,j}$ completely analogously to the non-Markovian case. We define $\tilde{B}(s) = (\mathbb{1}s - E)^{-1}D$ and obtain

$$\tilde{P}_i(s) = (\mathbb{1}s - E)^{-1}r_i$$
$$+ \sum_{k=1}^{\infty} \prod_{j=0}^{k-1} \tilde{B}(s + j\gamma)[\mathbb{1}(s + k\gamma) - E]^{-1}r_i \qquad (21)$$
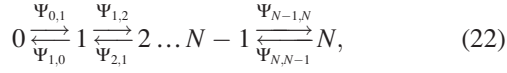
as the solution of Eq. (20).

These solutions for the Laplace transforms of the generalized and asymptotically Markovian master equations with
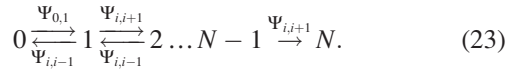
a transient, Eqs. (15) and (21), are not restricted to state-independent waiting-time distributions or rates. They also apply to random walks with space- or state-dependent waiting-time distributions and to arbitrary state networks.

III. THE PROBABILITY DENSITY OF THE FIRST-PASSAGE TIME FOR A LINEAR CHAIN OF STATES

A large class of stochastic processes, including all the examples mentioned in the introduction, are represented by linear state schemes like

$$0 \underset{\Psi_{1,0}}{\overset{\Psi_{0,1}}{\rightleftarrows}} 1 \underset{\Psi_{2,1}}{\overset{\Psi_{1,2}}{\rightleftarrows}} 2 \ldots N-1 \underset{\Psi_{N,N-1}}{\overset{\Psi_{N-1,N}}{\rightleftarrows}} N, \qquad (22)$$

which we consider from now on. The first-passage-time probability density $F_{0,N}(t)$ provides the probability of arrival for the first time in state N in $(t, t+dt)$ when the process started in state 0 at $t=0$. It can be determined by solving the master equations setting state 0 as the initial condition and considering the state N as absorbing, i.e., $\Psi_{N,N-1}(t, t-t') \equiv 0$.

$$0 \underset{\Psi_{i,i-1}}{\overset{\Psi_{0,1}}{\rightleftarrows}} 1 \underset{\Psi_{i,i-1}}{\overset{\Psi_{i,i+1}}{\rightleftarrows}} 2 \ldots N-1 \overset{\Psi_{i,i+1}}{\rightarrow} N. \qquad (23)$$

With this, $F_{0,N}(t)$ is given by the probability flux out of the state range from 0 to $N-1$

$$F_{0,N}(t) = -\frac{d}{dt} \sum_{k=0}^{N-1} P_{0,k}(t). \qquad (24)$$

We denote its Laplace transform by $\tilde{F}_{0,N}(s)$. The moments of the first-passage-time distribution are given by[15]

$$\langle t^n \rangle = (-1)^n \frac{\partial^n}{\partial s^n} \tilde{F}_{0,N}(s) \Big|_{s=0}. \qquad (25)$$

$F_{0,N}(t)$ captures not only the first-passage time $0 \to N$ but also, to a good approximation, transitions starting at states with indices larger than 0 (and $<N$), since, owing to the initial bias, the process quickly moves into state 0 first and then slowly starts from there.

A. Specification of the first passage problem for the generalized master equation

We specify the input for the generalized master equation of the non-Markovian system as

$$\Psi_{i,i+1} = \frac{\left(e^{-\alpha(t-t')} - e^{-\beta(t-t')}\right)\left(1 - e^{-\gamma t}\right)}{\frac{\beta - \alpha}{\alpha\beta} + \frac{(\beta-\alpha)(\epsilon+\gamma)(\delta+\gamma)}{\epsilon\delta(\alpha+\gamma)(\beta+\gamma)}}, \qquad (26)$$

$$\Psi_{i,i-1} = \frac{\left(e^{-\delta(t-t')} - e^{-\epsilon(t-t')}\right)\left(1 + e^{-\gamma t}\right)}{\frac{(\epsilon-\delta)(\alpha+\gamma)(\beta+\gamma)}{\alpha\beta(\epsilon+\gamma)(\delta+\gamma)} + \frac{\epsilon-\delta}{\epsilon\delta}}. \qquad (27)$$

The denominators in Eqs. (26) and (27) arise from the normalization to $C_{i,i+1}(t') + C_{i,i-1}(t')=1$ [Eq. (7)]. We use identical waiting-time distributions for all transitions $i \to i+1$ ($i > 0$) and all transitions $i \to i-1$ ($i > 0$). The process defined by Eqs. (26) and (27) has a strong bias toward 0 in the beginning and relaxes with rate γ to an approximately symmetric random walk. Figure 1 shows $\Psi_{i,i\pm1}$ and their development with increasing t'. The limit of $\gamma \ll \alpha, \beta, \epsilon, \delta$ illustrates the consequences of the transient. The $C_{i,i+1}$, $i > 0$ relax from 0 to an asymptotic value with rate γ, but the dwell times of individual states ($i \neq 0$) are essentially constant (Fig. 1).

There is only one transition away from 0. That changes the normalization to $C_{0,1}(t') = 1$ and we cannot use the form of Eqs. (26) and (27) for $\Psi_{0,1}$. We use instead

$$\Psi_{0,1} = \frac{\alpha_0\beta_0}{\beta_0 - \alpha_0 Z_0}\left[\left(e^{-\alpha_0(t-t')} - Z_0 e^{-\beta_0(t-t')}\right)\right.$$
$$\left. - e^{-\gamma t}\frac{(1-Z_0)(\epsilon_0+\gamma)}{\delta_0 - \epsilon_0}\left(\frac{\delta_0+\gamma}{\epsilon_0+\gamma}e^{-\delta_0(t-t')} - e^{-\epsilon_0(t-t')}\right)\right]. \qquad (28)$$
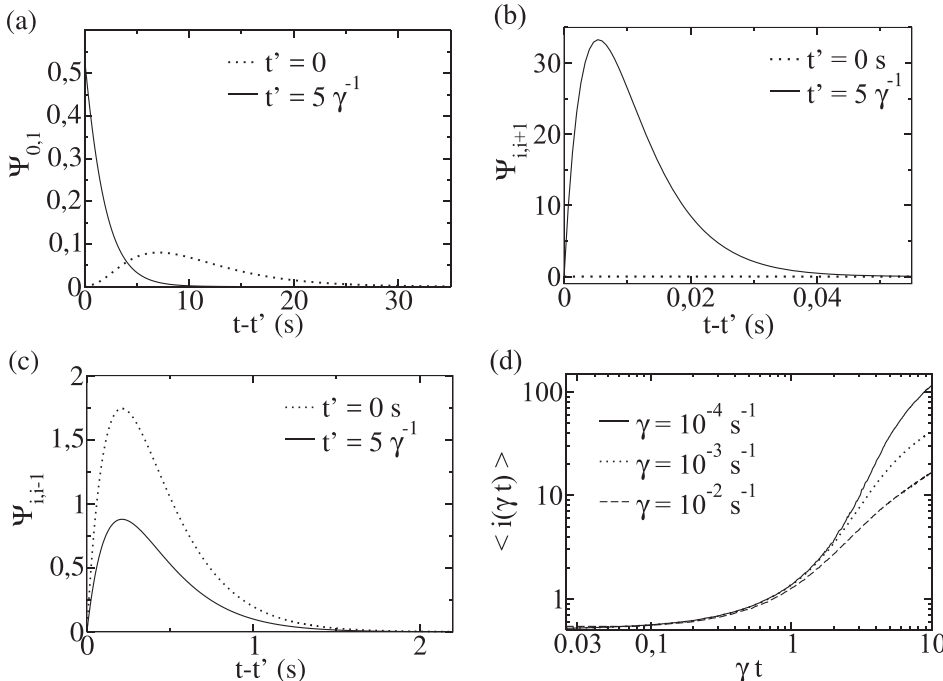

(a)

(b)

(c)

(d)

FIG. 1. Waiting-time distributions. (a) $\Psi_{0,1}$, the dwell time in state 0 decreases owing to the slow transient, but is always in the range of seconds. (b) $\Psi_{i,i+1}$ and (c) $\Psi_{i,i-1}$. Upon entering state i, the dependences of $\Psi_{i,i+1}$ and $\Psi_{i,i-1}$ on $t - t'$ with the large values of α and β used here entail transitions either to $i+1$ very early or to $i-1$ later [see the abscissa range in (b) and (c)]. (d) Simulation results for the average state index $\langle i(\gamma t)\rangle$. Since $C_{i,i-1}$ is initially close to 1, the process lingers around state 0 until $t \approx \gamma^{-1}$. When $C_{i,i-1}$ approaches $\frac{1}{2}$ at $t > \gamma^{-1}$, states further away from 0 with larger index i are also reached. Parameter values: (a) and (d) $\alpha_0 = 0.6$ s^{-1}, $\beta_0 = 1.07$ s^{-1}, $\delta_0 = 0.25$ s^{-1}, $\epsilon_0 = 0.225$ s^{-1}, and $Z_0 = 0.25$; (b), (c), and (d) $\alpha = 160$ s^{-1}, $\beta = 211$ s^{-1}, $\delta = 4.5$ s^{-1}, and $\epsilon = 5.0$ s^{-1}; (a)–(c) $\gamma = 0.01$ s^{-1}. The parameter values of (a)–(c) are the standard parameter set, which is used if not mentioned otherwise.

The transient here causes a decrease in the dwell time in state 0 (see Fig. 1).

With the definition in Eq. (6), the matrices $\tilde{G}(s)$ and $\tilde{H}(s)$ and the vector $\tilde{q}(s)$ [see Eq. (14)] specific to this problem are

$$\tilde{G}(s)_{1,2} = \tilde{g}_{0,1}(s),$$
$$\tilde{G}(s)_{2i,2i-1} = \tilde{G}(s)_{2i,2i+2}$$
$$= \tilde{g}_{i,i-1}(s), \quad i = 1, \ldots, N-2,$$
$$\tilde{G}(s)_{2i+1,2i-1} = \tilde{G}(s)_{2i+1,2i+2}$$
$$= \tilde{g}_{i,i+1}(s), \quad i = 1, \ldots, N-2,$$
$$\tilde{G}(s)_{2N-2,2N-3} = \tilde{g}_{N-1,N-2}(s),$$
$$\tilde{G}(s)_{2N-1,2N-3} = \tilde{g}_{N-1,N}(s),$$
$$\tilde{H}(s)_{1,2} = \tilde{h}_{0,1}(s),$$
$$\tilde{H}(s)_{2i,2i-1} = \tilde{H}(s)_{2i,2i+2}$$
$$= \tilde{h}_{i,i-1}(s), \quad i = 1, \ldots, N-2,$$
$$\tilde{H}(s)_{2i+1,2i-1} = \tilde{H}(s)_{2i+1,2i+2}$$
$$= \tilde{h}_{i,i+1}(s), \quad i = 1, \ldots, N-2,$$
$$\tilde{H}(s)_{2N-2,2N-3} = \tilde{h}_{N-1,N-2}(s),$$
$$\tilde{H}(s)_{2N-1,2N-3} = \tilde{h}_{N-1,N}(s),$$
$$\tilde{q}_1(s) = \tilde{\Psi}_{0,1}(s). \tag{29}$$

All other entries are equal to 0. Differences between the indices on the rhs and lhs arise from the definition of the vector $\tilde{I}(s)$ in Eq. (13), in which we deleted all fluxes identical to 0.

The Laplace transform of the first-passage-time distribution is [see Eq. (8)]

$$\tilde{F}_{0,N}(s) = \tilde{I}_{N-1,N}(s). \tag{30}$$

B. Specification of the first passage problem for the asymptotically Markovian master equation

We use the asymptotically Markovian rates

$$f_{i,i+1}(t) = \lambda(1 - e^{-\gamma t}), \quad f_{i,i-1}(t) = \lambda, \tag{31}$$

corresponding to $\lambda_{i,j} = \lambda$, $B_{i,i+1} = -1$, and $B_{i,i-1} = 0$ in Eq. (1). The process has also a strong initial bias for motion toward 0, $C_{i,i-1}(t'=0) > C_{i,i+1}(t'=0)$. It relaxes with rate γ to a symmetric random walk with $C_{i,i-1}(t'=\infty) = C_{i,i+1}(t'=\infty) = \frac{1}{2}$.

Specifically, for the first-passage problem, the matrices D and E [see Eq. (4)] are

$$E_{1,1} = -E_{1,2} = -E_{i,i\pm1} = -\lambda, \quad E_{i,i} = -2\lambda,$$
$$D_{1,1} = D_{i,i} = -D_{i,i-1} = \lambda, \quad i = 2, \ldots, N-1,$$

with all other entries being 0. The vector $\tilde{r}$ is equal to δ_{1i}, $i = 1, \ldots, N-1$. The Laplace transform of the first-passage-time distribution is

$$\tilde{F}_{0,N}(s) = \lambda\big[\tilde{P}_{0,N-1}(s) - \tilde{P}_{0,N-1}(s+\gamma)\big], \tag{32}$$

which is the transform of the probability flux $f_{N-1,N}(t)$ $P_{0,N-1}(t)$.

Figures 2(a) and 2(b) compare analytical results for the average first-passage time T with the results of simulations. The agreement is very good, thus confirming the solutions given by Eqs. (18) and (21). This confirmation by simulations is important, since there is no method of solving difference equations that guarantees a complete solution.

IV. SCALING OF THE AVERAGE FIRST-PASSAGE TIME WITH THE RELAXATION RATE

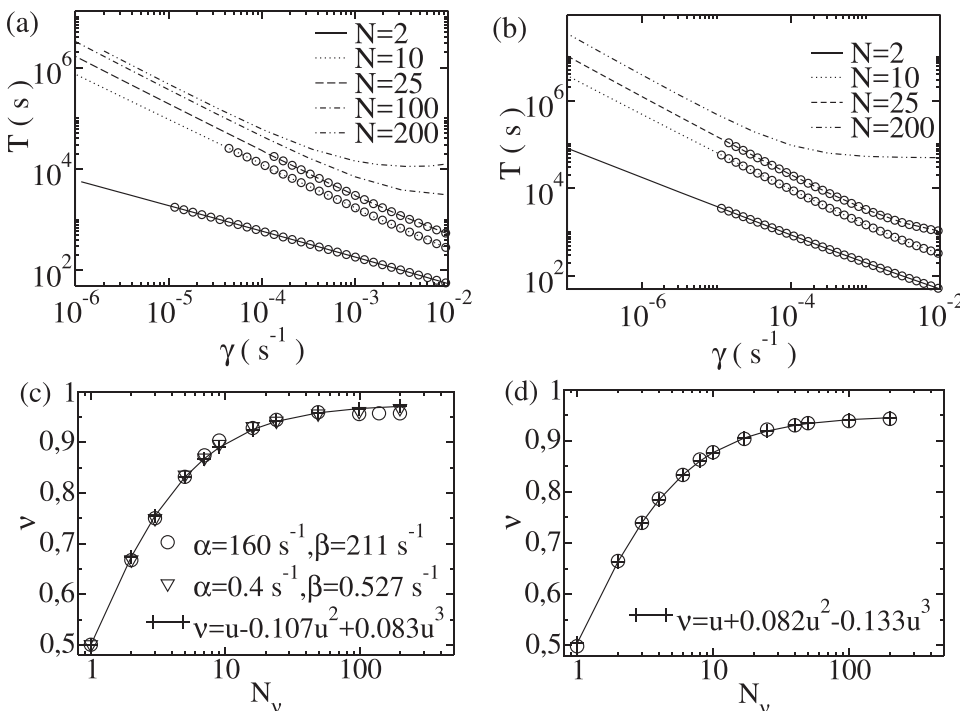Figure 2 shows results for the average first-passage time T across four orders of magnitude of the relaxation rate γ.

FIG. 2. The average first-passage time T has a power-law dependence on the relaxation rate γ of the initial transient of the form $\propto \gamma^{-\nu}$ for $\gamma \to 0$. (a) and (c) Results from solution of the generalized master equation (18) and Eqs. (26)–(28). (b) and (d) Results from solution of the asymptotically Markovian master equation (21) and Eq. (31) with $\lambda = 0.4$ s^{-1}. N_ν is the number of edges with identical waiting-time distributions. N_ν is equal to $N-1$ in (c) and to N in (d). The variable u in (c) and (d) is defined as $u = N_\nu/(N_\nu + 1)$. In (a) and (b), simulations (lines) are compared with analytical results (○). The relative deviations between analytical calculations and simulations are below 1%, i.e., within the precision which can be achieved with the number of 20 000–40 000 trajectories per data point used to calculate the average in simulations.

The results strongly suggest that T grows according to a power law $\gamma^{-\nu}$ with decreasing γ, if γ is sufficiently small. The exponent exhibits a simple dependence on the number N_ν of edges with identical waiting-time distributions. That number is equal to N for processes according to Eq. (31) and to $N - 1$ for processes obeying Eqs. (26)–(28), since the $0 \rightarrow 1$ transition is different there. The exponent ν depends to leading order on N_ν like $N_\nu/(N_\nu + 1)$. This applies to both the asymptotically Markovian and non-Markovian waiting-time distributions and to both parameter sets of waiting-time distributions simulated in the non-Markovian case.

The exponent ν is equal to $\frac{1}{2}$ for $N_\nu = 1$, as has previously been shown analytically for $f_{i,i\pm1}$ according to Eq. (31) (see Ref. 67, Chap. 5). The process is very unlikely to reach large N with a bias toward 0, even if this is only small. Hence, the random walk "waits" until the transient is over and symmetry of the transition rates has been reached [see Fig. 1(d)] and then goes to N. This waiting contributes a time $\propto \gamma^{-1}$ to T, and ν approaches 1 for large N_ν. However, even with the largest N and smallest values of γ ($\leq 10^{-6}$) in Fig. 2, ν reaches only about 0.975 and not 1. Hence, we could not finally establish, whether or how $\nu = 1$ is exactly reached for $N \rightarrow \infty$.

The average first-passage time for a symmetric random walk increases with N like $N(N - 1)$,[68] i.e., it is very long for large N. We see a contribution of the transient to T only if relaxation is slow enough for γ^{-1} to be comparable to this long time. Consequently, T is essentially independent of γ for large γ and large N [see $N = 200$ in Figs. 2(a) and 2(b)].

V. RESONANT LENGTH

The coefficient of variation CV [=standard deviation (SD)/average T] of the first-passage time reflects the relative fluctuations. Its dependence on the chain length N is illustrated in Fig. 3. CV increases monotonically with increasing γ. Its dependence on N is not monotonic. We find a pronounced minimum of CV(N) for small values of γ, where the minimal value is up to one order of magnitude smaller than CVs with $N = 1$ and with large N. This applies to the non-Markovian [Figs. 3(a), 3(c), and 3(d)] and asymptotically Markovian [Figs. 3(b) and 3(e)] cases, and both simulations [Figs. 3(c)–3(e)] and analytical results [Figs. 3(a) and 3(b)] show this behavior.

How can we get a heuristic understanding of the decrease in CV with decreasing γ and initially with increasing N? The lingering close to state 0 shown in Fig. 1(d) means that states with index i larger than 1 are not reached before a time $t \approx \gamma^{-1}$ with almost certainty. This initial part of the process contributes to T but little to SD. Hence, its
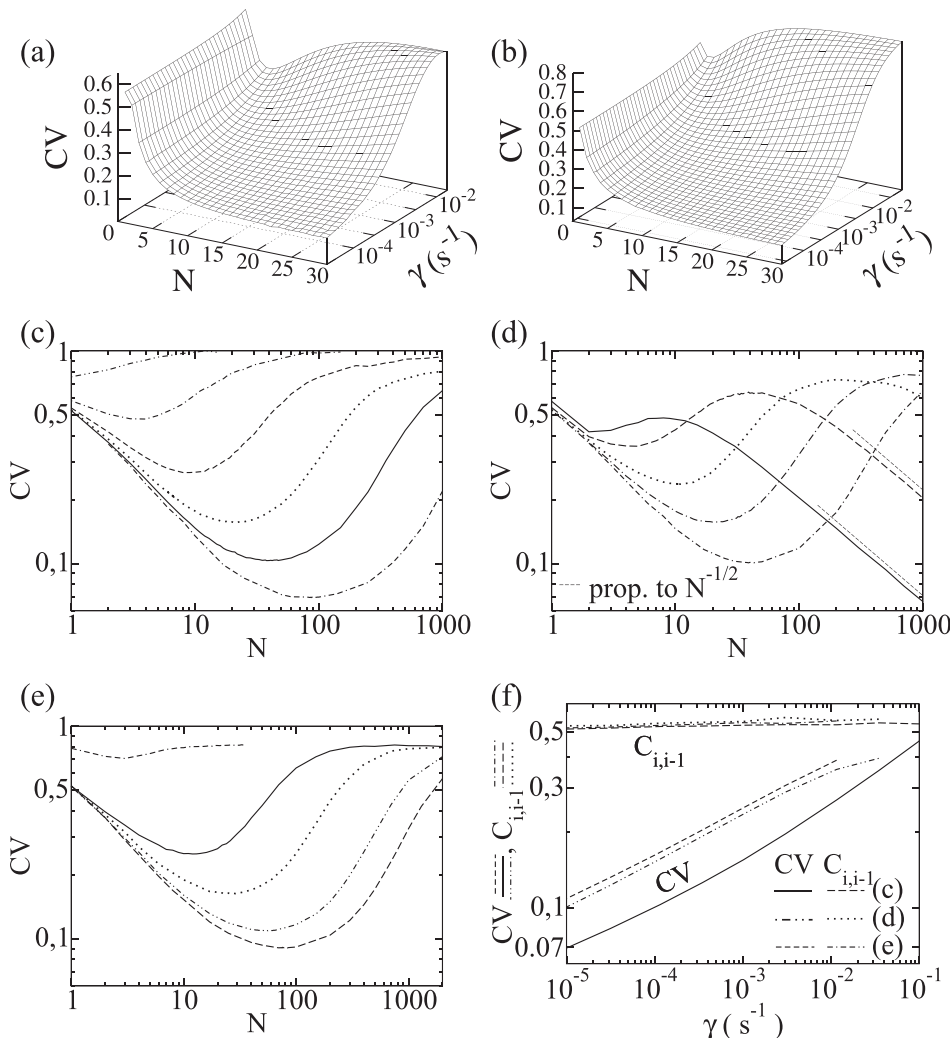

FIG. 3. The coefficient of variation CV shows a pronounced minimum in its dependence on the chain length N. (a) Analytical results using the solution of the generalized master equation (18) and Eqs. (26)–(28). (b) Analytical results using the solution of the asymptotically Markovian master equation (21) and Eq. (31). (c) and (d) Simulations using Eqs. (26)–(28). (e) Simulations using Eq. (31). (f) Properties of the minima of the CV as a function of the relaxation rate γ. The splitting probability $C_{i,i-1}(t' = T)$ at the minimum changes only slightly over four orders of magnitude of γ [between 0.515 and 0.565 in (c), 0.531 and 0.564 in (d), and 0.516 and 0.555 in (e)]. The dependence of the minimal CV on γ shown in (f) is well fitted by $\gamma^{0.181}$ in the asymptotically Markovian case (e) and by $\gamma^{0.186}$ for $\gamma < 2 \times 10^{-3}$ s^{-1} for the parameter values in (d), but deviates from a power law for the values in (c). Parameter values: (a) $\alpha = 0.4$ s^{-1} and $\beta = 0.5275$ s^{-1}; (b) $\lambda = 0.4$ s^{-1}; (c) from top to bottom: $\gamma = 1$, 1.156×10^{-1}, 1.156×10^{-2}, 1.015×10^{-3}, 1.156×10^{-4}, and 10^{-5} s^{-1} and $C_{i,i-1}(t' = \infty) \gtrsim \frac{1}{2}$; (d) $\alpha = 0.4$ s^{-1}, $\beta = 0.5275$ s^{-1}, and from top to bottom: $\gamma = 0.1$, 1.156×10^{-2}, 1.015×10^{-3}, 1.156×10^{-4}, and 10^{-5} s^{-1} and $C_{i,i-1}(t' = \infty) \lesssim \frac{1}{2}$; (e) $\lambda = 0.4$ s^{-1}, $C_{i,i-1}(t' = \infty) = \frac{1}{2}$, $\gamma = 1$, $10^{-3}, 10^{-4}, 10^{-5}$, and $10^{-5.5}$ s^{-1}.

growth with decreasing γ and (initially) increasing N decreases CV. Additionally, the standard deviation is determined by the rates and splitting probabilities at the end of the transient, which are more favorable for reaching N than the splitting probabilities at the beginning. It is therefore less affected than the average by the γ values. This also causes a decrease in CV with decreasing γ.

To gain more insight into the N dependence of CV, we look at processes with constant transition rates and a symmetric process with transient rates but constant splitting probabilities $C_{i,i-1} = C_{i,i+1} = \frac{1}{2}$ [see Eq. (A1)]. The permanently symmetric process exhibits only a very shallow minimum, and the minimal value of CV appears to be independent of γ [Fig. 4(a): discrete case]. Processes with constant transition rates exhibit decreasing CV with decreasing $C_{i,i-1}$[68] [Fig. 4(b)]. However, this decrease is minor and does not explain the data in Fig. 3 in the range $C_{i,i-1} \geq \frac{1}{2}$ covered by the transient.

The comparison shows that the dynamics of the splitting probabilities provide the major part of the reduction in CV with increasing N in Fig. 3. The splitting probability $C_{i,i-1}$ relaxes from 1 to its asymptotic value set by the parameters of the process. The larger the value of N, the later is the absorbing state reached and the smaller is the value of $C_{i,i-1}$ when it is reached. As long as $C_{i,i-1}(t' = T)$ decreases sufficiently rapidly with increasing N, so does CV. At values of N such that $\gamma T \gtrsim 2$, the decrease in $C_{i,i-1}(t' = T)$ is negligible, and CV starts to rise again with increasing N toward its large-N value.

These considerations suggest that the N with minimal CV could be fixed by a specific value of the splitting probability. This value of $C_{i,i-1}$ cannot be smaller than $\frac{1}{2}$, since we would expect a monotonically decreasing CV in that regime [the $N^{-\frac{1}{2}}$ regime in Fig. 3(d)]. Since this should hold also for minima with $N \gg 1$, this value of $C_{i,i-1}$ also cannot be much larger than $\frac{1}{2}$, since T would then diverge. This is confirmed by the results shown in Fig. 3(f). The splitting probability $C_{i,i-1}(t' = T)$ at the minimum changes by less than 8% over four orders of magnitude of γ and is slightly larger than $\frac{1}{2}$. Hence, CV starts to rise again when the length N is so large that the average first-passage time is long enough for $C_{i,i-1}(t' = T)$ to approach the symmetric limit.[69]

The value of CV($N = \infty$) depends on γ in the case with non-Markovian waiting-time distributions. It is 1 for large γ values, since the asymptotic splitting probability $C_{i,i-1}(t' = \infty)$ is larger than $\frac{1}{2}$ [Fig. 3(c); see also Fig. 4(b)]. A reference value is the CV of a symmetric random walk with constant transition rates and large N, which is equal to $\sqrt{2/3}$.[68] CV($N = \infty$) is approximately equal to $\sqrt{2/3}$ for small values of γ, since $C_{i,i-1}(t' = \infty) \approx \frac{1}{2}$ applies in that case [Fig. 3(c)]. CV($N = \infty$) is exactly $\sqrt{2/3}$ with asymptotically Markovian waiting-time distributions [Fig. 3(e)].

The parameter values in Fig. 3(d) entail $C_{i,i-1}(t' = \infty) \lesssim \frac{1}{2}$. The process has a bias toward N and we see the well-known behavior CV(N) $\propto N^{-\frac{1}{2}}$ for large N. The onset of the $N^{-\frac{1}{2}}$ behavior moves to smaller N with increasing values of γ until finally the minimum of the CV is lost. We found minima if $\gamma^{-1} \gtrsim$ (four times the average state dwell time), but we have not determined a precise critical value.
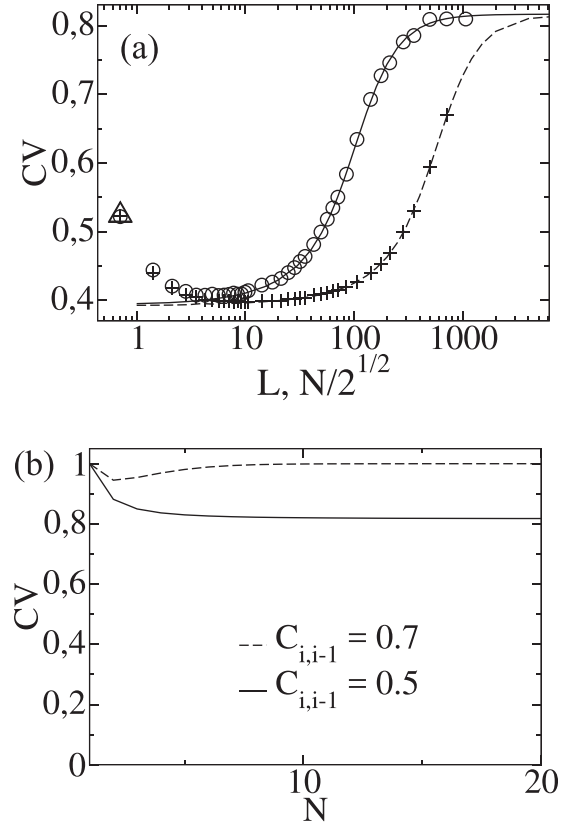

FIG. 4. (a) The coefficient of variation CV shows a shallow minimum in its dependence on the chain length N with processes that are discrete and always symmetric (symbols), but not for the continuous symmetric case (lines), which is the solution of the Fokker–Planck equation (A2). The symbols $+$ and $\circ$ show results from simulations using Eq. (A1). The calculations used $\lambda = 0.4$ s^{-1} (all), and $\gamma = 10^{-4}$ s^{-1} ($\circ$, full line) and $\gamma = 3.6 \times 10^{-6}$ s^{-1} ($+$, dashed line). The value of the CV at the minimum is essentially unaffected by the change in the value of γ. The $\triangle$ marks the analytical result with $N = 1$ for both discrete cases, which are indistinguishable at the resolution of the plot and are in agreement with the simulations. The continuous large-L and discrete large-N results agree very well. (b) CV with constant transition rates calculated using the equations of Jouini and Dallery.[68] CV $\geq \sqrt{2/3}$ holds for $C_{i,i-1} \geq \frac{1}{2}$.

The transition from the CV of $\Psi_{0,1}$ to CV($N = \infty$) for large values of γ is monotonic in Fig. 3(c) for the asymptotically non-Markovian case. The asymptotically Markovian system exhibits a minimum even for large γ values [$\gamma \approx \lambda$: Fig. 3(e)]. However, it is comparably shallow and is in line with the results of Jouini and Dallery for systems without transient[68] [Fig. 4(b)].

VI. DISCUSSION AND CONCLUSION

A. (Generalized) master equation with exponential time dependence of rates and waiting-time distributions

In general, stochastic processes occur in changing environments or may be subjected to control. The corresponding mathematical description is provided by (generalized) master equations with time-dependent coefficients. The analytical solution of these equations is complicated even in the simplest case [see Eq. (A8)].[70] The Laplace-transform approach is not applicable in general, but the exponential time dependences of Eqs. (2), (8), and (9) do allow the transform to be

performed on them, leading to difference equations in Laplace space. The solutions of these equations are given by Eqs. (18) and (21), respectively. To the best of our knowledge, this is a novel (and efficient) method of solving the generalized master equation with this type of time dependence in the kernel or the master equation with this type of time-dependent rates.

The solutions [Eqs. (18) and (21)] also apply in the case of state schemes more complicated than scheme (22). It is only necessary to make appropriate changes to the definitions of $\tilde{H}(s)$ and $\tilde{G}(s)$ or of D and E. Hence, we can use the method presented here to investigate the dynamics of complicated networks in a transient. This is of interest for studies of ion-channel dynamics,[53,54,71] transport in more than one spatial dimension, gene regulatory networks, and many other applications. Many quantities of interest in these investigations are moments of first-passage type and thus can be calculated from the derivatives of the Laplace transforms. Some of these calculations might require knowledge of the probability time dependence $P_{i,j}(t)$, i.e., the residues of $\tilde{P}_{i,j}(s)$. In many cases, determination of these residues will be only slightly more complicated than for the system without transient, since all terms arising from the transient involve the same factors, but with shifted argument, together with the matrix $\tilde{H}(s)$. In general, if we know the set of residues $\{S_0\}$ of the Laplace transform of the system without transient and the matrix $\tilde{H}(s)$, we can immediately write down the residues of the Laplace transform of the system with transient by shifting $\{S_0\}$ by integer multiples of γ. This allows easy generalization of many results and might be of particular interest for renewal theory.[15,72]

B. The average first-passage time

The average first-passage time decreases with increasing relaxation rate according to a power law, if the transient is sufficiently slower than the time scale of the individual steps (Fig. 2). The exponent depends on the chain length to leading order like $-N/(N+1)$. Remarkably, this behavior has been found for substantially different parameters in both the asymptotically non-Markovian and asymptotically Markovian cases and therefore appears to be rather universal.

C. Resonant length

Transients can substantially reduce the coefficient of variation. We have found a monotonic decrease in CV with decreasing γ when the relaxation rate is slow compared with state transition rates. CV exhibits a minimum in its dependence on the chain length N (Fig. 3) if the transient is slow compared with state dynamics. This minimum exists for both asymptotically Markovian and non-Markovian discrete systems. At a time-scale separation between the state transition rates and the transient of about 10^6, the CV at the minimum is reduced by about one order of magnitude compared with CV($N=1$).

Exploiting our results for control purposes, we can use a transient if more precise arrival timing at the outcome of a process is desired. Applying a transient that relaxes a bias toward 0 reduces CV. In the context of charge carrier transport, such a transient could be realized by a time-dependent electric field. If we include the rising part of CV(N) beyond the minimum in our consideration and consider all CVs smaller than CV($N=1$) as reduced, we may still see a reduction of CV even if the average first-passage time is an order of magnitude longer than γ^{-1}. Hence, the initial transient may have surprisingly long-term consequences and is therefore a rather robust method for CV reduction. Additionally, or if a transient is given, the state and step number can be used for optimizing the precision of arrival time. The optimum may also be at smaller lengths than that of the non-optimized process; i.e., optimization of precision may even lead to acceleration.

D. How can negative feedback robustly reduce noise in timing?

Most studies investigating the effect of negative feedback have focused on amplitude noise—we are looking at noise in timing. Timing noise substantially reduces information transmission in communication systems. Variability in timing and protein copy numbers in gene expression or cell differentiation causes cell variability.[37,73] Therefore, many studies have investigated the role of noise in gene regulatory networks and have found that immediate negative feedback is not suitable for reducing timing noise.[74–76] This agrees with our results for large γ values. The recovery from negative feedback corresponds to the transient in our present study. Therefore, our results show that slow recovery from negative feedback is a robust means of timing noise reduction.

Negative feedback terminating the excited state is a constitutive element of many systems generating sequences of pulses or spikes, such as oscillating chemical reactions,[77,78] the electrical membrane potential of neurons,[79] the sinoatrial node controlling the heart beat,[80] the tumor suppressor protein p53,[81,82] Ca^{2+} spiking in eukaryotic cells,[83–85] cAMP concentration spikes in *Dictyostelium discoideum* cells, and other cellular signaling systems.[86,87]

In particular, our results apply to noisy excitable spike generators in cells, where single molecular events or sequences of synaptic inputs form a discrete chain of states toward the threshold. In addition to the examples from membrane potential spike generation,[88] Ca^{2+} spiking and p53 pulse sequences have been shown to be noise-driven excitable systems.[82,84,85,89] The information content of frequency-encoding spiking increases strongly with decreasing CV of spike timing.[90] A value of the coefficient of variation between 0.2 and 1.0 has been measured for the sequence of interspike intervals of intracellular Ca^{2+} signaling.[84,85,91–93] Hence, CV is decreased compared with that of a Poisson process and even compared with that for first passage of a symmetric random walk. The experimental data are also compatible with the finding that the slower the recovery from negative feedback, the lower is CV.[84,85,91–93] This strongly suggests that this ubiquitous cellular signaling system uses the mechanism of noise reduction described here to increase information transmission.

Optimal noise amplitudes minimize the CV of interspike intervals in noisy excitable systems,[40,94–97] which has been

termed coherence resonance. Our results define the conditions of optimal CV reduction in terms of system properties—an optimal number of steps from the inhibited state to the excitation threshold during slow recovery. At the same time, our results shed light on new aspects of coherence resonance, and indeed may indicate that a more fundamental phenomenon underlies it. Since we believe excitable systems to be one of the most important applications of our results, we have chosen the term *resonant* length.

Coming back to the widely used graphic example, what can the drunkard learn from our results? If he chooses a pub at the right distance from home, he will arrive home sober and relatively in time for breakfast.

ACKNOWLEDGMENTS

APPENDIX A: THE SYMMETRIC ASYMPTOTICALLY MARKOVIAN CASE AND ITS CONTINUUM LIMIT

The permanently symmetric case with a transient is defined by

$$f_{i,i\pm1}(t) = \lambda(1 - e^{-\gamma t}). \tag{A1}$$

Its continuum limit on a domain of length L (with spatial coordinate x) satisfies

$$\frac{\partial P(x,t)}{\partial t} = 2\lambda(1 - e^{-\gamma t})\frac{\partial^2 P(x,t)}{\partial x^2}. \tag{A2}$$

The Fokker–Planck equation (A2) can be solved after applying a time transformation $t \to \tau$

$$\tau(t) = 2\int_0^t f_{i,i\pm1}(t')\,dt' = 2\lambda\left(t + \frac{e^{-\gamma t}}{\gamma} - \frac{1}{\gamma}\right). \tag{A3}$$

The boundary and initial conditions, $P(L,t) = 0$, $\partial P(x,t)/\partial x|_{x=0} = 0$, and $P(x,0) = \delta(x)$ specify the first-passage problem. We find

$$P(x,\tau) = \frac{2}{L}\sum_{n=0}^{\infty}\cos(k_n x)e^{-k_n^2\tau}, \tag{A4}$$

where $k_n = \pi(2n+1)/(2L)$. The ith moment of the first-passage time is given by

$$\langle t^i \rangle = \int_0^{\infty} t^i F(t)\,dt, \tag{A5}$$

$$F(t) = -\frac{d}{dt}\int_0^L P(x,\tau(t))\,dx. \tag{A6}$$

With $a_n = 2\lambda k_n^2/\gamma$, we obtain

$$\langle t \rangle = \frac{4}{\pi\gamma}\sum_{n=0}^{\infty}\frac{(-1)^n}{2n+1}e^{a_n}a_n^{-a_n}\Gamma(a_n, a_n), \tag{A7}$$

where $\Gamma(y,x)$ is the lower incomplete gamma function. The second moment is

$$\langle t^2 \rangle = \frac{32L^4}{\lambda^2\pi^5}\sum_{n=0}^{\infty}\frac{(-1)^n}{(2n+1)^5}e^{a_n}$$
$$\times {}_2F_2(\{a_n, a_n\}; \{a_n + 1, a_n + 1\}; -a_n), \tag{A8}$$

where ${}_2F_2$ is a hypergeometric function. Results for CV are shown in Fig. 4(a). In the continuous case, CV does not exhibit a minimum in its dependence on the length L. Interestingly, CV at small L is very close to the minimum value of the discrete case.

The a_n are small for $L \gg \lambda/\gamma$. Therefore, in that limit, we can approximate the incomplete Γ function and hypergeometric function by

$$\Gamma(a_n, a_n) \approx a_n^{a_n - 1}e^{-a_n},$$
$$e^{a_n}{}_2F_2(\{a_n, a_n\}; \{a_n + 1, a_n + 1\}; -a_n) \approx 1,$$

and find

$$\mathrm{CV}(L \gg \lambda/\gamma) \approx \sqrt{\frac{5}{3}\frac{L^4}{\lambda^2}\frac{\lambda^2}{L^4} - 1} = \sqrt{\frac{2}{3}}, \tag{A9}$$

i.e., CV approaches monotonically the value of a symmetric random walk with constant transition rates for large L.

APPENDIX B: NUMERICAL METHODS

Evaluation of Eqs. (18) and (21): If N is large and the ratio between the fastest state transition rate and the relaxation rate γ is larger than 10^4, high precision of the numerical calculations is required for the use of Eqs. (18) and (21). A *priori* known values like $\tilde{I}_{N-1,N}^0(s=0) = 1$ can be used to monitor the precision of the calculations. The matrix products become very large at intermediate values of $j\gamma$ during the summation in Eqs. (18) and (21), and their sign alternates such that two consecutive summands nearly cancel. Intermediate summands are of order larger than 10^{17}, and thus we face loss of significant figures even with the numerical floating-point number format long double. We used Arb, a C numerical library for arbitrary-precision interval arithmetic,[98] to circumvent this problem. It allows for arbitrary precision in calculations with Eqs. (18) and (21). Computational speed is the only limitation with this library and has determined the parameter range for which we established analytical results. We were able to go to a time-scale separation of $\approx 10^{-6}$ using this library. We calculated moments with a relative precision of 4×10^{-4}. Computations eligible for the C++ long double format ($\gamma \geq 10^{-3}\,s^{-1}$) take seconds on a laptop computer. Arbitrary precision computations take between 90 min and 10 days.

These numerical problems occur, if there is a range of s where some eigenvalues of $\tilde{A}(s)$ are outside the unit circle. We mentioned in Sec. II B that the solutions in this case still converge, if the eigenvalues are within the unit circle for large s ($s > s_1$). This holds for $\gamma > 0$. We also know the solution for $\gamma = 0$ [Eq. (19)]. However, in the limit $\gamma \to 0$ we may face infinitely many factors with eigenvalues outside the unit circle. We could not demonstrate in general that they are compensated by the factors with small eigenvalues at $s + k\gamma > s_1$

in Eq. (18), but could demonstrate it down to a time scale ratio individual steps/relaxation of 10^{-6}. Nonetheless, the solution at $\gamma = 0^+$ might be different from the solution at $\gamma = 0$.

Simulation method: We use simulations for comparison with the analytic solutions and for systems with large N. The $\Psi_{l,j}(t, t - t')$ are functions only of t for a given t'. Since t' is the time when the process moved into state l, it is always known. The simulation algorithm generates in each iteration the cumulative distribution $\int_{t'}^{t} d\theta \sum_{i=1}^{N_{\text{out}}^{(l)}} \Psi_{l,j_i}(\theta, \theta - t')$ and then draws the time t_{tr} for the next transition. The specific transition is chosen from the relative values $\Psi_{l,j_k}(t_{\text{tr}}, t_{\text{tr}} - t') / \sum_{i=1}^{N_{\text{out}}^{(l)}} \Psi_{l,j_i}(t_{\text{tr}}, t_{\text{tr}} - t')$ by a second draw. We verified the simulation algorithm by comparison of simulated and calculated stationary probabilities [Eq. (C4)], splitting probabilities at a variety of t' values, simulations without recovery ("$\gamma = \infty$") and the comparisons in Fig. 2. We used at least 20 000 sample trajectories to calculate moments and up to 160 000 to determine the location of the minima of CV.

The outcome of a comparison with respect to computational efficiency between the evaluation of Eqs. (18) and (21) and simulations strongly depends on the desired precision. With the precisions achieved with Eqs. (18) and (21) (4×10^{-4}), simulations with a sufficient number of sample trajectories for the same precision of moments would be orders of magnitude slower than the summation of the matrix products.

APPENDIX C: THE STATIONARY PROBABILITIES

The stationary probabilities are reached for $t \to \infty$. This entails $\Psi_{i,i\pm1}(t, t - t') = \Psi_{i,i\pm1}^{\infty}(t - t') = g_{i,i\pm1}(t - t')$. We start from the idea that the stationary probability P_i of being in state i is equal to the ratio of the total average time T_i spent in i divided by the total average time for large t

$$P_i = \frac{T_i}{\sum_{j}^{N} T_j}. \tag{C1}$$

T_i is equal to the number N_i of visits to state i multiplied by the average dwell time t_i in i

$$P_i = \frac{t_i N_i}{\sum_{j}^{N} t_j N_j}. \tag{C2}$$

Each visit to state i starts with a transition to i. The average number of transitions into i is equal to the number of visits to its neighboring states multiplied by the probability that the transition out of the neighboring states is toward i. With the splitting probabilities $C_{i,i\pm1}(t = \infty)$ denoted by $C_{i,i\pm1}$, the N_i obey

$$N_i = C_{i-1,i} N_{i-1} + C_{i+1,i} N_{i+1}. \tag{C3}$$

Dividing by the total number of visits $\sum_{j=0}^{N} N_j$, we get

$$n_i = C_{i-1,i} n_{i-1} + C_{i+1,i} n_{i+1}, \tag{C4}$$

$$1 = \sum_{j=0}^{N} n_j, \tag{C5}$$

$$P_i = \frac{t_i n_i}{\sum_{j=0}^{N} t_j n_j}. \tag{C6}$$

We write Eq. (C4) in matrix form, $\mathbb{M}\mathbf{n} = \mathbb{0}$, with

$$M_{i,i\pm1} = -\tilde{g}_{i\pm1,i}(0), \tag{C7}$$

$$M_{i,i} = 1, \tag{C8}$$

and all other entries 0. We checked for $N = 2$, 3, and 4 that $\det \mathbb{M} = 0$ holds. Equation (C4) determines n only up to a common factor, which is then fixed by Eq. (C5).

The average dwell times t_i in the states are initially affected by the recovery from negative feedback, but are constant at large t. They have contributions $t_{i,i\pm1}$ from both transitions to $i \pm 1$, with weights set by $C_{i,i\pm1}$

$$t_i = C_{i,i+1} t_{i,i+1} + C_{i,i-1} t_{i,i-1}. \tag{C9}$$

$C_{i,i\pm1} t_{i,i\pm1} = -(\partial/\partial s)\tilde{g}_{i,i\pm1}|_{s=0}$ holds owing to the normalization of the $\Psi_{i,i\pm1}$. This leads finally to

$$t_i = -\frac{\partial}{\partial s}\left(\tilde{g}_{i,i-1} + \tilde{g}_{i,i+1}\right)\Big|_{s=0}. \tag{C10}$$

To give a specific example, the stationary-state probabilities for $N = 2$ are

$$\mathbb{P} = \frac{1}{(\partial/\partial s)\left(C_{1,0}\tilde{g}_{0,1} + \tilde{g}_{1,0} + \tilde{g}_{1,2} + C_{1,2}\tilde{g}_{2,1}\right)}$$
$$\times \begin{pmatrix} C_{1,0}(\partial/\partial s)\tilde{g}_{0,1} \\ (\partial/\partial s)\left(\tilde{g}_{1,0} + \tilde{g}_{1,2}\right) \\ C_{1,2}(\partial/\partial s)\tilde{g}_{2,1} \end{pmatrix}\Bigg|_{s=0}.$$

[1] Q.-H. Wei, C. Bechinger, and P. Leiderer, "Single-file diffusion of colloids in one-dimensional channels," Science **287**, 625–627 (2000).

[2] M. Chupeau, O. Bénichou, and R. Voituriez, "Cover times of random searches," Nat. Phys. **11**, 844 (2015).

[3] T. Guérin, N. Levernier, O. Bénichou, and R. Voituriez, "Mean first-passage times of non-Markovian random walkers in confinement," Nature **534**, 356–359 (2016).

[4] A. Molini, P. Talkner, G. Katul, and A. Porporato, "First passage time statistics of Brownian motion with purely time dependent drift and diffusion," Physica A: Stat. Mech. Appl. **390**, 1841–1852 (2011).

[5] D. Panja, "Anomalous polymer dynamics is non-Markovian: Memory effects and the generalized Langevin equation formulation," J. Stat. Mech.: Theory Exp. **2010**, P06011 (2010).

[6] T. Turiv, I. Lazo, A. Brodin, B. I. Lev, V. Reiffenrath, V. G. Nazarenko, and O. D. Lavrentovich, "Effect of collective molecular reorientations on Brownian motion of colloids in nematic liquid crystal," Science **342**, 1351–1354 (2013).

[7] V. Démery, O. Bénichou, and H. Jacquin, "Generalized Langevin equations for a driven tracer in dense soft colloids: Construction and applications," New J. Phys. **16**, 053032 (2014).

[8] D. Ernst, M. Hellmann, J. Kohler, and M. Weiss, "Fractional Brownian motion in crowded fluids," Soft Matter **8**, 4886–4889 (2012).

[9] S. D. Baranovskii, "Theoretical description of charge transport in disordered organic semiconductors," Phys. Status Solidi B **251**, 487–525 (2014).

[10] R. Metzler and J. Klafter, "The random walk's guide to anomalous diffusion: A fractional dynamics approach," Phys. Rep. **339**, 1–77 (2000).

[11] A. Blumen, J. Klafter, and I. Sokolov, "Fractional kinetics," Phys. Today **55**(11), 48–54 (2002).

[12]H. Hofmann and F. A. Ivanyuk, "Mean first passage time for nuclear fission and the emission of light particles," Phys. Rev. Lett. **90**, 132701 (2003).

[13]I. M. Sokolov and J. Klafter, "From diffusion to anomalous diffusion: A century after Einstein's Brownian motion," Chaos **15**, 026103 (2005).

[14]M. F. Shlesinger, "Mathematical physics: Search research," Nature **443**, 281–282 (2006).

[15]N. van Kampen, *Stochastic Processes in Physics and Chemistry* (North-Holland, Amsterdam, 2001).

[16]I. Oppenheim, K. E. Shuler, and G. H. Weiss, *Stochastic Processes in Chemical Physics: The Master Equation* (MIT Press, 1977).

[17]O. Bénichou, C. Chevalier, J. Klafter, B. Meyer, and R. Voituriez, "Geometry-controlled kinetics," Nat. Chem. **2**, 472 (2010).

[18]H. C. Berg, *Random Walks in Biology* (Princeton University Press, 1993).

[19]M. Gazzola, C. J. Burckhardt, B. Bayati, M. Engelke, U. F. Greber, and P. Koumoutsakos, "A stochastic model for microtubule motors describes the *in vivo* cytoplasmic transport of human adenovirus," PLOS Comput. Biol. **5**, e1000623 (2009).

[20]P. C. Bressloff and J. M. Newby, "Stochastic models of intracellular transport," Rev. Mod. Phys. **85**, 135–196 (2013).

[21]I. V. Ivanov, X. Qian, and R. Pal, *Emerging Research in the Analysis and Modeling of Gene Regulatory Networks* (IGI Global, Hershey, PA, 2016).

[22]L. O. Scott, "Pricing stock options in a jump-diffusion model with stochastic volatility and interest rates: Applications of Fourier inversion methods," Math. Finance **7**, 413–426 (1997).

[23]J. M. Steele, *Stochastic Calculus and Financial Applications*, edited by B. Rozovskii and M. Yor, Stochastic Modelling and Applied Probabilty, Vol. 45 (Springer, 2000).

[24]M. L. Mayo, E. J. Perkins, and P. Ghosh, "First-passage time analysis of a one-dimensional diffusion-reaction model: Application to protein transport along DNA," BMC Bioinf. **12**, S18 (2011).

[25]R. B. Winter and P. H. von Hippel, "Diffusion-driven mechanisms of protein translocation on nucleic acids," Biochemistry **20**, 6929–6948 (1981).

[26]O. G. Berg, R. B. Winter, and P. H. von Hippel, "Diffusion-driven mechanisms of protein translocation on nucleic acids. 1. Models and theory," Biochemistry **20**, 6929–6948 (1981).

[27]A. D. Riggs, S. Suzuki, and S. Bourgeois, "Lac repressor-operator interaction. I. Equilibrium studies," J. Mol. Biol. **48**, 67–83 (1970).

[28]A. D. Riggs, S. Bourgeois, and M. Cohn, "The lac repressor-operator interaction. III. Kinetic studies," J. Mol. Biol. **53**, 401–417 (1970).

[29]N. Shimamoto, "One dimensional diffusion of proteins along DNA: Its biological and chemical significance revealed by single-molecule measurements," J. Biol. Chem. **274**, 15293–15296 (1999).

[30]M. Albert, G. Haack, C. Flindt, and M. Büttiker, "Electron waiting times in mesoscopic conductors," Phys. Rev. Lett. **108**, 186806 (2012).

[31]H. Scher and M. Lax, "Stochastic transport in a disordered solid. I. Theory," Phys. Rev. B **7**, 4491–4502 (1973).

[32]T. Britton, "Stochastic epidemic models: A survey," Math. Biosci. **225**, 24–35 (2010).

[33]*First-Passage Phenomena and Their Applications*, edited by S. Redner, R. Metzler, and G. Oshanin (World Scientific Publishing Co. Pte. Ltd., 2014).

[34]S. Redner, *A Guide to First-Passage Processes* (Cambridge University Press, 2001).

[35]S. Condamin, O. Bénichou, V. Tejedor, R. Voituriez, and J. Klafter, "First-passage times in complex scale-invariant media," Nature **450**, 77–80 (2007).

[36]M. F. Shlesinger, "First encounters," Nature **450**, 40–41 (2007).

[37]S. Hormoz, Z. S. Singer, J. M. Linton, Y. E. Antebi, B. I. Shraiman, and M. B. Elowitz, "Inferring cell-state transition dynamics from lineage trees and endpoint single-cell measurements," Cell Syst. **3**, 419–433.e8 (2016).

[38]J. Garca-Ojalvo and L. Schimansky-Geier, "Excitable structures in stochastic bistable media," J. Stat. Phys. **101**, 473–481 (2000).

[39]M. Kostur, X. Sailer, and L. Schimansky-Geier, "Stationary probability distributions for Fitzhugh-Nagumo systems," Fluctuation Noise Lett. **03**, L155–L166 (2003).

[40]B. Lindner, J. Garcia-Ojalvo, A. Neimann, and L. Schimansky-Geier, "Effects of noise in excitable systems," Phys. Rep. **392**, 321–424 (2004).

[41]M. Falcke, M. Bär, H. Engel, and M. Eiswirth, "Traveling waves in the co oxidation on pt(110): Theory," J. Chem. Phys. **97**, 4555–4563 (1992).

[42]J. Keener and J. Sneyd, *Mathematical Physiology* (Springer, New York, 1998).

[43]A. C. Scott, "The electrophysics of a nerve fiber," Rev. Mod. Phys. **47**, 487–533 (1975).

[44]X. Pei, K. Bachmann, and F. Moss, "The detection threshold, noise and stochastic resonance in the Fitzhugh-Nagumo neuron model," Phys. Lett. A **206**, 61–65 (1995).

[45]M. Cross and P. Hohenberg, "Pattern formation outside of equilibrium," Rev. Mod. Phys. **65**, 851 (1993).

[46]A. Mikhailov, *Foundations of Synergetics*, Springer Series in Synergetics, Vols. 1 and 2 (Springer, 1994).

[47]W. Ebeling and R. Feistel, *Physik der Selbstorganisation und Evolution* (Akademieverlag Berlin, 1986).

[48]T. Franosch, M. Grimm, M. Belushkin, F. M. Mor, G. Foffi, and L. Forro, "Resonances arising from hydrodynamic memory in Brownian motion," Nature **478**, 85–88 (2011).

[49]M. Esposito and K. Lindenberg, "Continuous-time random walk for open systems: Fluctuation theorems and counting statistics," Phys. Rev. E **77**, 051119 (2008).

[50]M. Albert, D. Chevallier, and P. Devillard, "Waiting times of entangled electrons in normal-superconducting junctions," Physica E **76**, 209–215 (2016).

[51]J. Koch, M. E. Raikh, and F. von Oppen, "Full counting statistics of strongly non-ohmic transport through single molecules," Phys. Rev. Lett. **95**, 056801 (2005).

[52]B. Hille, *Ion Channels of Excitable Membranes*, 3rd ed. (Sinauer Assoicates, Inc., Publishers, Sunderland, MA, USA, 2001).

[53]P. Cao, G. Donovan, M. Falcke, and J. Sneyd, "A stochastic model of calcium puffs based on single-channel data," Biophys. J. **105**, 1133–1142 (2013).

[54]J. Sneyd, M. Falcke, J. F. Dufour, and C. Fox, "A comparison of three models of the inositol trisphosphate receptor," Prog. Biophys. Mol. Biol. **85**, 121–140 (2004).

[55]K. Thurley, L. F. Wu, and S. J. Altschuler, "Modeling cell-to-cell communication networks using response-time distributions," Cell Systems **6**, 355–367.e5 (2018).

[56]V. Kenkre, "Generalization to spatially extended systems of the relation between stochastic Liouville equations and generalized master equations," Phys. Lett. A **65**, 391–392 (1978).

[57]P. Hänggi and P. Talkner, "First-passage time problems for non-Markovian processes," Phys. Rev. A **32**, 1934–1937 (1985).

[58]J. Masoliver, K. Lindenberg, and B. J. West, "First-passage times for non-Markovian processes: Correlated impacts on bound processes," Phys. Rev. A **34**, 2351–2363 (1986).

[59]R. Metzler, E. Barkai, and J. Klafter, "Deriving fractional Fokker-Planck equations from a generalised master equation," EPL (Europhys. Lett.) **46**, 431 (1999).

[60]$\Psi_{j,k}(t,0)$=0 applies if the system enters the lumped state always at a "microscopic" state through which it cannot exit.

[61]J. H. Davies, P. Hyldgaard, S. Hershfield, and J. W. Wilkins, "Classical theory for shot noise in resonant tunneling," Phys. Rev. B **46**, 9620–9633 (1992).

[62]V. M. Kenkre, E. W. Montroll, and M. F. Shlesinger, "Generalized master equations for continuous-time random walks," J. Stat. Phys. **9**, 45–50 (1973).

[63]E. W. Montroll and H. Scher, "Random walks on lattices. IV. Continuous-time walks and influence of absorbing boundaries," J. Stat. Phys. **9**, 101–135 (1973).

[64]A. I. Burshtein, A. A. Zharikov, and S. I. Temkin, "Non-Markov theory of sudden modulation," Theor. Math. Phys. **66**, 166–173 (1986).

[65]A. V. Chechkin, R. Gorenflo, and I. M. Sokolov, "Fractional diffusion in inhomogeneous media," J. Phys. A: Math. Gen. **38**, L679 (2005).

[66]I. Sokolov and J. Klafter, "Continuous-time random walks in an oscillating field: Field-induced dispersion and the death of linear response," Chaos, Solitons Fractals **34**, 81–86 (2007).

[67]G. Dupont, M. Falcke, V. Kirk, and J. Sneyd, *Models of Calcium Signalling*, edited by S. Antman, L. Greengard, and P. Holmes, Interdisciplinary Applied Mathematics, Vol. 43 (Springer, 2016).

[68]O. Jouini and Y. Dallery, "Moments of first passage times in general birth–death processes," Math. Methods Oper. Res. **68**, 49–76 (2008).

[69]The minima of the CV are less correlated with a specific value of the product γT, since γT at the minima changes by about 20% in Fig. 3(c) and about 80% in Figs. 3(d) and 3(e) across the γ-range.

[70]A. Skupin and M. Falcke, "Statistical analysis of calcium oscillations," Eur. Phys. J. Spec. Top. **187**, 231–240 (2010).

[71]E. Gin, M. Falcke, L. E. Wagner, D. I. Yule, and J. Sneyd, "A kinetic model of the inositol trisphosphate receptor based on single-channel data," Biophys. J. **96**, 4053–4062 (2009).

[72]D. Cox, *Renewal Theory* (Methuen & Co, 1970).

[73]E. Yurkovsky and I. Nachman, "Event timing at the single-cell level," Briefings Funct. Genomics **12**, 90–98 (2013).

[74]S. Kontogeorgaki, R. J. Sánchez-García, R. M. Ewing, K. C. Zygalakis, and B. D. MacArthur, "Noise-processing by signaling networks," Sci. Rep. 7, 532 (2017).

[75]M. Hinczewski and D. Thirumalai, "Noise control in gene regulatory networks with negative feedback," J. Phys. Chem. B 120, 6166–6177 (2016).

[76]K. R. Ghusinga, J. J. Dennehy, and A. Singh, "First-passage time approach to controlling noise in the timing of intracellular events," Proc. Natl. Acad. Sci. U. S. A. 114, 693–698 (2017).

[77]J. F. Totz, R. Snari, D. Yengi, M. R. Tinsley, H. Engel, and K. Showalter, "Phase-lag synchronization in networks of coupled chemical oscillators," Phys. Rev. E 92, 022819 (2015).

[78]M. Falcke and H. Engel, "Influence of global coupling through the gas phase on the dynamics of CO oxidation on Pt(110)," Phys. Rev. E 50, 1353–1359 (1994).

[79]E. Kandel, J. Schwartz, and T. Jessel, Principles of Neural Science (Appleton & Lange, Norwalk, Connecticut, 1991).

[80]A. Pohl, A. Wachter, N. Hatam, and S. Leonhardt, "A computational model of a human single sinoatrial node cell," Biomed. Phys. Eng. Express 2, 035006 (2016).

[81]K. H. Vousden and D. P. Lane, "p53 in health and disease," Nat. Rev. Mol. Cell Biol. 8, 275–283 (2007).

[82]G. Mönke, E. Cristiano, A. Finzel, D. Friedrich, H. Herzel, M. Falcke, and A. Loewer, "Excitability in the p53 network mediates robust signaling with tunable activation thresholds in single cells," Sci. Rep. 7, 46571 (2017).

[83]M. Falcke, "Reading the patterns in living cells—The Physics of Ca^{2+} signaling," Adv. Phys. 53, 255–440 (2004).

[84]A. Skupin, H. Kettenmann, U. Winkler, M. Wartenberg, H. Sauer, S. C. Tovey, C. W. Taylor, and M. Falcke, "How does intracellular Ca^{2+} oscillate: By chance or by the clock?," Biophys. J. 94, 2404–2411 (2008).

[85]K. Thurley, S. C. Tovey, G. Moenke, V. L. Prince, A. Meena, A. P. Thomas, A. Skupin, C. W. Taylor, and M. Falcke, "Reliable encoding of stimulus intensities within random sequences of intracellular Ca^{2+} spikes," Sci. Signal. 7, ra59 (2014).

[86]A. Goldbeter, Biochemical Oscillations and Cellular Rhythms (Cambridge University Press, Cambridge, 1996).

[87]M. Falcke and H. Levine, "Pattern selection by gene expression in Dictyostelium discoideum," Phys. Rev. Lett. 80, 3875–3878 (1998).

[88]J. Grewe, A. Kruscha, B. Lindner, and J. Benda, "Synchronous spikes are necessary but not sufficient for a synchrony code in populations of spiking neurons," Proc. Natl. Acad. Sci. U. S. A. 114, E1977–E1985 (2017).

[89]K. Thurley and M. Falcke, "Derivation of Ca^{2+} signals from puff properties reveals that pathway function is robust against cell variability but sensitive for control," Proc. Natl. Acad. Sci. U. S. A. 108, 427–432 (2011).

[90]A. Skupin and M. Falcke, "From puffs to global Ca^{2+} signals: How molecular properties shape global signals," Chaos 19, 037111 (2009).

[91]S. Dragoni, U. Laforenza, E. Bonetti, F. Lodola, C. Bottino, R. Berra-Romani, G. Carlo Bongio, M. P. Cinelli, G. Guerra, P. Pedrazzoli, V. Rosti, F. Tanzi, and F. Moccia, "Vascular endothelial growth factor stimulates endothelial colony forming cells proliferation and tubulogenesis by inducing oscillations in intracellular Ca^{2+} concentration," Stem Cells 29, 1898–1907 (2011).

[92]P. Cao, X. Tan, G. Donovan, M. J. Sanderson, and J. Sneyd, "A deterministic model predicts the properties of stochastic calcium oscillations in airway smooth muscle cells," PLoS Comput. Biol. 10, e1003783 (2014).

[93]J. Lembong, B. Sabass, and H. A. Stone, "Calcium oscillations in wounded fibroblast monolayers are spatially regulated through substrate mechanics," Phys. Biol. 14, 045006 (2017).

[94]P. Jung and G. Mayer-Kress, "Spatiotemporal stochastic resonance in excitable media," Phys. Rev. Lett. 74, 2130–2133 (1995).

[95]A. Pikovski and J. Kurths, "Coherence resonance in a noise-driven excitable system," Phys. Rev. Lett. 78, 775–778 (1997).

[96]H. Gang, T. Ditzinger, C. Z. Ning, and H. Haken, "Stochastic resonance without external periodic force," Phys. Rev. Lett. 71, 807–810 (1993).

[97]V. Beato, I. Sendiña-Nadal, I. Gerdes, and H. Engel, "Coherence resonance in a chemical excitable system driven by coloured noise," Philos. Trans. R Soc. London A 366, 381–395 (2008).

[98]F. Johansson, "Arb: Efficient arbitrary-precision midpoint-radius interval arithmetic," IEEE Trans. Comput. 66, 1281–1292 (2017).